UCRL- 92367
PREPRINT

MAGNETIC INSULATION

Marco S. Di Capua

THIS PAPER WAS PREPARED FOR SUBMITTAL TO
IEEE Transactions
on Plasma Science

March 7, 1985

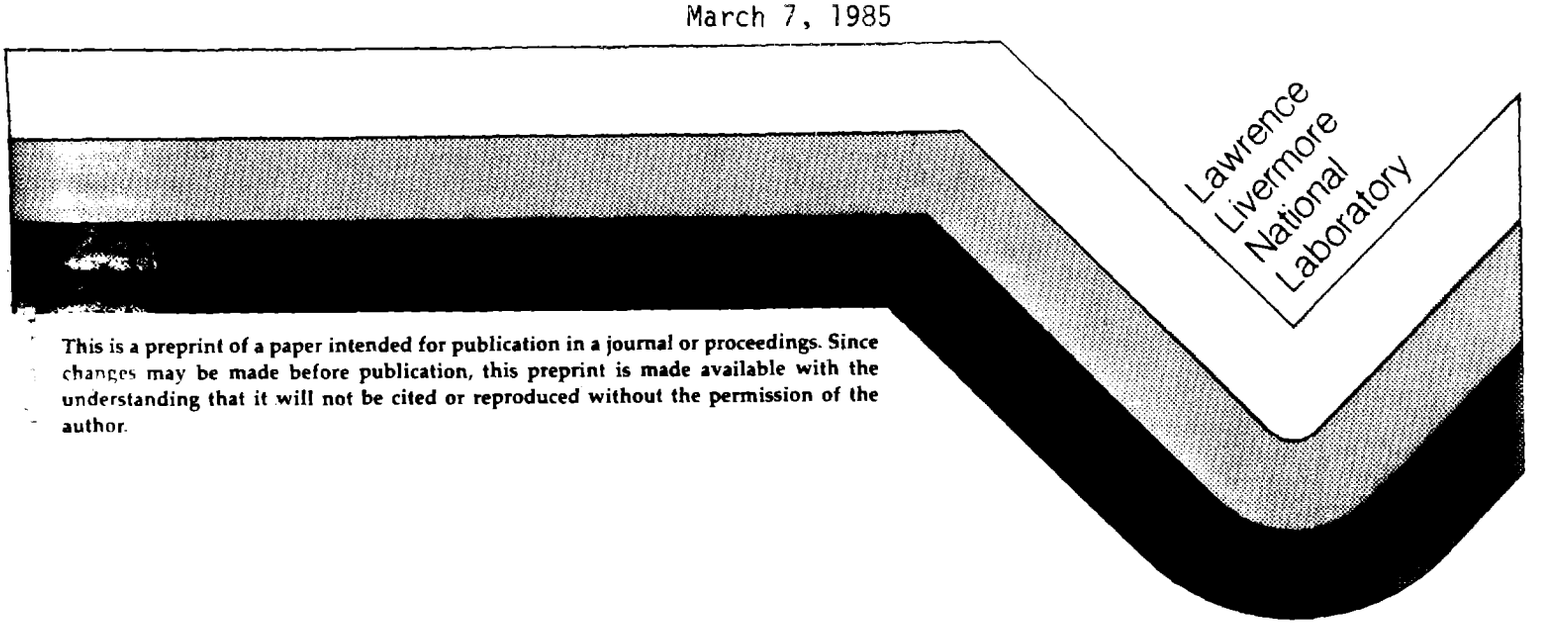

MAGNETIC INSULATION*

Marco S. Di Capua
Lawrence Livermore National Laboratory
P.O. Box 808
Livermore, CA 94550

ABSTRACT

In the magnetic insulation process in transmission lines, the magnetic field associated with the power flow at very high Poynting vectors cuts off the electron flow from the negative to the positive conductor. This paper examines magnetic insulation in regions of changing impedance, discusses the results of self-consistent calculations, introduces the concept of convolutes, examines magnetic insulation in the feeds of imploding plasma load drivers, and provides a brief overview of plasma closure of the gap in magnetically insulated vacuum transmission lines.

*Work performed under the auspices of the U.S. Department of Energy by the Lawrence Livermore National Laboratory under contract number W-7405-ENG-48. Also supported in part by Defense Nuclear Agency at Physics International Company, 2700 Merced Street, San Leandro, CA 94577.

1. INTRODUCTION

In a 1983 paper that appeared in this same journal [1], the author reviewed the subject of magnetic insulation as applied to the delivery of large Poynting vectors to particle beam loads in relativistic electron beam accelerators. The reference discussed stationary flows in constant impedance regions (single particle, laminar flow, quasi-laminar flow, and flow with arbitrary momenta descriptions), nonstationary flows (laminar approximations, minimum energy operating point, equivalent circuit simulations, particle-in-cell simulations), and transitions (laminar flow analysis and transition designs).

This paper describes some recent analysis of flow with arbitrary momenta; presents single particle descriptions of transitions in magnetically insulated vacuum transmission lines (MITLs); discusses results obtained with self-consistent calculations where the effects of space charge are accounted for; discusses post hole convolutes; reviews magnetic insulation in MITLs driving imploding plasma loads; and provides a brief overview of gap closure in MITLs.

2. FLOWS WITH ARBITRARY MOMENTA

Recently, Mendel [2] has presented an analysis of magnetic insulation that rests upon a minimum number of assumptions founded upon well established experimental facts. Throughout this discussion, the subscripts a and c refer to the anode and cathode, respectively.

a) The cathode is a space charge limited emitter so that the electric field at the cathode $E_c = 0$.

b) The anode is not a space charge limited ion emitter. If it were a space charge limited emitter, MITLs would not work since the magnetic fields are not large enough to trap the ion flow.

c) The electron pressure at the anode is negligible compared to the field pressure.

d) In equilibrium flow, the electron cloud travels parallel to the electrodes without being accelerated towards either. Pressure balance therefore requires for the electric field at the anode E_a,

$$E_a^2 = c^2 \left(B_a^2 - B_c^2\right)$$

where $\int_{a,c} B \cdot d\ell = \mu_o I_{a,c}$.

e) The electron drift velocity $\bar{V}$ is

$$\bar{V} = c\left(\frac{I_a - I_c}{I_a + I_c}\right)^{1/2} .$$

f) The magnetic force at the anode must equal or exceed the electric force to prevent electrons from striking the anode. Consequently,

$$I_a = I_c \left(1 + FeV_m/m_o c^2\right) .$$

The parameter F depends on V_m and the spread of momenta. Typical values of F ($0.2 < F < 1.0$) appear in Fig. 2 of Mendel's [3] work.

g) The extent d_m of the sheath into the gap d in a planar geometry of width w is

$$2\pi \frac{I_c}{I_\alpha} \frac{d_m}{w} = G \left(\frac{2eV_m}{m_o c^2} \right)^{1/2} \quad .$$

The parameter G, which is a weak function of V_m, the potential at the edge of the sheath and the spread of momenta in the distributions, appears in Fig. 2 of Mendel's [3] work and has a typical range of $0.7 < A < 1.4$; $I_\alpha = (m_o c^2/e)(2\pi/\mu_o c)$.

h) Invoking pressure balance across the flow the expression for the anode potential is:

$$\frac{eV_o}{m_o c^2} = \frac{I_c}{I_\alpha g} \left(\left(\frac{I_a}{I_c} \right)^2 - 1 \right)^{1/2} + \frac{\frac{I_a}{I_c} - 1}{F} \left(1 - G \left(2F \left(\frac{I_a}{I_c} + 1 \right) \right)^{1/2} \right) \quad .$$

Fortuitously, the second term on the right is not very sensitive to the choice of F and G, so both parameters can be set to 1 without causing a large error in the calculation. Hence,

$$\frac{eV_o}{m_o c^2} \simeq \frac{I_c}{I_\alpha g} \left(\left(\frac{I_a}{I_c} \right)^2 - 1 \right)^{1/2} + \left(\frac{I_a}{I_c} - 1 \right) \left(1 - \left(2 \left(\frac{I_a}{I_c} + 1 \right) \right) \right)^{1/2} \quad .$$

Accurate measurements of the anode current I_a and the cathode current I_c can therefore yield the anode potential V_o. Mendel [3] compared the anode potential predicted by this method to measurements obtained in MITLs by Di Capua [4] and VanDevender [5] and found excellent agreement. Rosenthal [6] has applied this technique to obtain the voltage in the MITLs of the PBFA I accelerator on a routine basis.

Useful curves relating I_a and I_c for a fixed anode potential resulting from the foregoing analysis appear in Fig. 4 of Ref. [2]. The curves, reproduced in Fig. 1, correspond to F = G = 1. The quantity Z is the same as $Z_0 = 60\Omega\, g^{-1}$ defined in Ref. [7] where g is the geometrical factor. The greater of I_1 and I_2 is the anode current I_a and the lesser is the cathode current I_c. The curves uniquely establish a value of anode potential, appearing as the label in each curve for a choice of Z and measured values of I_1 and I_2. Similarly, following the dashed lines these curves may be used to establish the anode and cathode currents resulting from an applied anode potential. The assumption is, of course, that the MITL operates at the minimum energy condition [8].

3. NUMERICAL SIMULATIONS OF STATIONARY FLOWS IN REGIONS OF CHANGING IMPEDANCE

Calculations to predict the behavior of electrons in the insulator-magnetically insulated transmission line (MITL) transition (Type I) regions and in the transition between the MITL and the load (Type II) are important from an MITL design standpoint.

In the early days of particle beam fusion, Poukey [9] developed extensive numerical simulations of stationary flows to predict the behavior of focusing diodes. These simulations solved the electric and magnetic fields in a region, taking into account the presence of space charge. Results were current density as well as space charge density as a function of time and position. While these simulations did not account for propagation of electromagnetic waves in the region, they did allow an evolution of the electron flow in time.

Applicability of these codes to the solution of magnetic insulation problems is limited. Wave propagation, which cannot be neglected in practical structures, develops the electron flow and establishes the boundary/initial conditions required to start the problem. Consequently, even stationary flow simulations require the solution of the time dependent problem first. Otherwise, they require the application of some ad-hoc boundary conditions.

There are two useful particle simulation methods to study transitions. One of them takes the solutions to the vacuum electrostatic potential problem and solves the equations of motion of individual electrons in the vacuum region. By following trajectories of individual electrons, in what amounts to a generalization of the critical current concept, one can establish which geometries or transitions are likely to cause loss of electrons to the anode. Rigorously, these solutions are only valid for test charges which do not alter the field distribution outside the cathode sheath. Space charge effects are important inside the sheath and, therefore, the solutions are not valid inside the sheath. Drift theory is very useful to interpret with resulting trajectories as shown by Clauser [10]. Genuario [11] has applied calculations of this type to design MITLs used for power concentration.

To illustrate the effect of a transition on electron orbits, we have calculated electron orbits in Type I and Type II transitions using the technique described in Ref. [1]. The electron orbits appear in Figs. 2 and 3. The geometry is coaxial, and positive bias current flows in the cathode in the z-direction. The results for a Type I transition appear in Fig. 2. The anode potential V_0 = 1 MV, the cathode bias current I_b = -54.30 kA and the geometrical factor before the transition are identical to those of Fig. 2(d)

of Ref. [1], so electrons graze the 0.25 MV equipotential. The anode potential and bias current do not change through the transition. We chose the geometrical factor g = 2.29 after the transition to get orbits of electrons born after the transition to just graze the anode. The equipotentials appear in Fig. 2(a). In this transition, $\partial\phi/\partial z > 0$. This fact is essential to the interpretation of the trajectories as we shall see below.

We follow the approach of Creedon [12] and describe the motion of an electron in the anode cathode region by a Lagrangian function $L = \gamma m_0 c^2 - q\phi + q\vec{v} \cdot \vec{A}$ where ϕ is the potential, $\vec{v}$ is the velocity and $\vec{A}$ is the magnetic vector potential. The equation of motion of the z velocity component is $d/dt\ (\partial L/\partial v_z) = \partial L/\partial z$ and $\partial L/\partial v_z = P_z = \gamma m_0 v_z + qA_z$ is the canonical momentum in the z direction. Hence, $\partial L/\partial z = -q\ \partial\phi/dz$.

In a Type I transition, $\partial\phi/\partial z > 0$, - q is positive for an electron so $\partial L/\partial z > 0$ and therefore $dP_z/dt > 0$. Since $P_z = 0$ before the transition, $P_z > 0$ after the transition. A_z and v_z are zero at the cathode, $|v_z| > 0$ by energy conservation and $A_z > 0$ by definition. Since $\gamma m_0 v_z - eA_z > 0$, then $v_z > 0$ over the whole orbit and by energy conservation the electrons can no longer reach the cathode. Hence, electron orbits which were common cycloids before the transition become curtate cycloids after the transition, as shown in Fig. 2(b). To complete the discussion we show, in Fig. 2(c), orbits of electrons launched after the transition. These orbits, due to the choice of g, I_b and V_0 just graze the anode.

For a Type II transition, we have chosen to flare out the 0.25 MV equipotential of Fig. 2(d) of Ref. [1]. Equipotentials for this transition appear in Fig. 3(a). For this transition, $\partial\phi/\partial z < 0$. An argument parallel to

the one presented above shows that $\gamma m_o v_z - eA_z < 0$ after the transition. In this case, depending on the value of A_z, v_z can be positive or negative. By considering the shape of $\gamma(r)$ and $A_z(r)$ and energy conservation arguments, Mendel [13] shows that for negative momenta, v_z is negative at the bottom turning point and v_z is positive at the upper turning point. Hence, the orbits become prolate cycloids. These are the orbits which appear in Fig. 3(b). Figure 3(c) shows that electrons born after the transition are very well trapped due to the comparatively small geometrical factor. Notice, however, that the electrons launched before the transition have orbits which extend further into the gap then those of electrons launched after the transition.

Illustrative as they may be, results from calculations such as these must be used with caution. The presence of space charge and electron currents in the gap change $A_z(r)$ and $\phi(r)$ from the vacuum values which affects the electron trajectories.

To introduce some of the effects due to space charge in the gap, Neau [14] assumes that the laminar flow model describes locally the position of the sheath, the fields within it, and the fields between the sheath and the anode. He integrates the relativistic equations of motion of an electron test particle in these fields and obtains the momentum the electron acquires in its motion through the transition. The calculations determine how much momentum the electron acquires in transitions of different geometries. He finds that a gradually tapering transition introduces a broader distribution of momenta, that the momentum increases through the transition, and that the increase is less than in a transition where vacuum fields alone are present. He concludes

that this broader distribution may be responsible for the better injection efficiency observed by VanDevender [15] in transitions with a more gentle taper.

Desjarlais [16] investigated with the MASK code [17] the effect, on the electron sheath flow, of a step discontinuity in the gap of a MITL. The results were that discontinuities in the cathode surface cause a larger increase in the sheath thickness than discontinuities in the anode surface. In the simulations, the electron sheath quickly departs from laminar flow as soon as it encounters a step or protrusion.

The behavior of the electron flow may be explained by the conservation of canonical momentum. The step introduces a component of the electric field in the direction of the flow. The electrons decelerate and their loss of momentum produces orbits that no longer reach the cathode and have a retrograde velocity at their lower point. The sheath is therefore displaced into the A-K gap, as shown in Fig. 2(b). In the case of periodic structures, repeated interactions with the protrusion further deteriorate the electron sheath to the point that electrons scatter towards the anode.

4. CONVOLUTE DESIGNS

Many particle beam fusion design concepts require the interconnection in vacuum of several magnetically insulated vacuum transmission lines which feed a central load. The task of the designer is difficult because, in such a connection, abrupt transitions, and complicated electric and magnetic field geometries which may include magnetic field zeroes, cannot be avoided. To complicate matters even further, it is necessary to consider the possibility

that the power pulses from different modules may not all arrive to the convolute at the same time.

As part of the initial design effort for PBFA I, Di Capua [4] tested a convolute conceived by Champney [18] which rotated the electric field vector 90° from a horizontal to a vertical direction. This convolute would join several triplate MITLs to a disk feed. This convolute, tested at ~ 1 MV, provided excellent current transport with a positive and a negative center conductor. About 10% of the total current flowed in the space charge at the convolute location.

Spence [19] proposed a post-hole convolute to join to disk or coax feeds in the vicinity of a load. This type of convolute was conceived to merge the power from two sides of a tridisk or triaxial vacuum feed into a bidisk or simple coax feed. Figure 4 shows an 180° section of a model of a post-hole convolute for a tridisk feed. The cathode is common to the top and bottom MITLs. The posts connect the top and bottom anodes, passing through holes in the cathode. The imploding plasma load is strung between the cathode and bottom anode. After the convolute, the bottom anode carries the sum of the currents on both sides. The cathode current in the upper feed passes through the edge of the holes and joins the current in the bottom feed.

Crow [20] tested a post-hole convolute to convert the coaxial output from a PBFA MITL into the triaxial output required for an ion diode. In this convolute, four pins about 3 mm in diameter penetrate the positive electrode through circular holes about 1.5 cm in diameter. The 2.9 Ω load overmatched the 4.8 Ω self-limiting impedance of the power feeding MITL so the voltage on the convolute was approximately 1 MV. At this voltage, the transport

efficiency was 100%. The space charge, due to the impedance mismatch, comprised only a very small fraction of the total current. Therefore, the losses were low.

Crow [21] has also tested a different kind of convolute in which he connects two coaxial MITLs to a triplate disk feed. The center conductors connect to the center disk. The outer conductors are split and connect to the top and bottom feeds. The center conductor was negative in these tests. Data obtained with synchronous pulses into loads in the matched to short circuit range, showed very little losses either in the transitions themselves, or in the disk region which faces the split ground conductor of the coaxes. This is a low magnetic field region which caused some concern about the design. With a load impedance above the matched self-limiting impedance of the MITLs, there was some damage where the central disk faces the "cuts" in the coaxes.

Jitter between modules is unavoidable in a large accelerator system. The early pulse arriving at the convolute, by partly propagating through the convolute into the other transmission lines, could have two undesirable effects. One effect would be the creation of plasmas on the surface of the electrodes of the MITLs which could short the gap upon arrival of the later pulses. The second effect would be to subtract from the current and add to the electric field of the later pulse.

Crow [21] systematically delayed one of the pulses which fed the two-line convolute to investigate these phenomena. He found that in the load impedance range between short circuit and matched loads, the energy in the early pulse which propagated in the other line was insufficient to degrade the propagation of the late pulse. Less than one-third of the current of the early pulse

propagated upstream in the other transmission line. It appears that this current was not sufficient to disrupt magnetic insulation and that the predictions of Seidel [22] were rather pessimistic.

Crow [6] tested an 18-line triplate to disk convolute with positive center conductors to adapt PBFA-I for ion diode experiments. Preliminary results indicated that there were no losses in the transitions or at the disk edge.

A different type of convolute adds the electric vector from propagating pulses instead of adding currents as the ones we have described so far do. Two pulses of opposite polarity propagating in two sets of MITLs add in the convolute to deliver a pulse of double amplitude and the same current. This convolution connects the positive MITLs in parallel, the negative MITLs in parallel, and the load in series between the positive and negative connections.

Quintenz [23] performed a simulation of this convolute with a 2-D approximation to the 3-D problem using the solution in one part of the region as an input to the solution in other parts of the region. In this convolute, the MITL ground is at a -2 MV potential with respect to the anode and emission from the ground electrode could cause problems. The simulations showed that the electron flow comprised only about 5% of the total current and that electron flow near the -4 MV electrode was well trapped.

Turman [6] performed tests on such a convolute, driven by two positive and two negative output lines. Early tests confirmed that the prediction of current loss from the ground electrode was correct. Modifications of the geometry reduced this loss to a level that could not be detected by x-ray

detectors or through hardware damage. The current transport of 600 kA comprised more than 70% of the MITL output. Operations in opposite polarity were judged equally successful.

5. MAGNETIC INSULATION IN MITLS DRIVING IMPLODING PLASMA LOADS

The production of high energy density Z-pinch plasmas with super power generators [24] has opened a rapidly developing chapter in the subject of magnetic insulation. While MITLs which drive imploding plasma loads share much of the physics we have discussed to this point, there are significant differences which merit special attention.

In the design of the vacuum stage of imploding plasma load drivers, a conflict exists between a low MITL inductance which requires a large g and the trapping criterion in the MITL which requires a small g. Another conflict exists between the small gaps required for a low inductance, and the large gaps required for a long impedance lifetime. The perimeter of the liquid dielectric required to deliver the power from the accelerator sets the third requirement. Large powers need large perimeters (hence, large radii) which conflicts with the requirement of a low inductance feed.

Why low inductance? Because sub-ohm generators with pulse durations in the 100 ns range need inductive time constants $\tau = L/Z_g$ of 30 ns implying, for example, a 15 nH inductance for the combination of feed and Z-pinch load applied to a 0.5 Ω generator. Shorter pulse durations and lower impedances compound the problem at first sight. However, shorter pulse durations do alleviate the difficulties caused by gap closure.

5.1. ANALYSIS OF MITLS DRIVING IMPLODING PLASMA LOADS

The MITLs for this application are commonly called vacuum feeds or simply feeds. The analysis techniques we have described so far must be applied with caution to feeds which drive imploding plasma loads. In the first place, most feeds which drive imploding plasma loads are a Type I transition which leads into a Type II transition with a very short, if any, constant impedance transmission line in between. Moreover, in the vicinity of the load, the magnetic field gradients in these feeds become significant and ∇B drifts become important. In the second place, one would predict that current losses would be substantial until the anode current $I(t) = L^{-1} \int_0^t V d\tau$ becomes sufficient for the self-magnetic field to trap the electron flow. Thus, the conditions in these feeds never become stationary even though $\tau c/\ell > 1$. Thirdly, to minimize the inductance, the gaps in these feeds are comparable to the distances covered by plasmas during the power pulse, so that plasma motion can no longer be ignored. Plasma motion in the feed is aggravated by the soft x-ray environment in the vicinity of the imploding plasma load which contributes to plasma formation on the electrodes. In this section we examine the MITL analysis techniques we have introduced before in the context of imploding plasma loads and point out their applicability and limitations.

5.1.1. Analytical Approximations

The characteristics of Fig. 4 of Ref. [1] are useful to establish whether a feed is magnetically insulated or not. We illustrate the approach in Fig. 5. On the top left we show the voltage which we apply across an inductor L. The inductor consists of the feed and the Z-pinch load. For simplicity,

we assume that the load inductance does not change with time. The current which appears at the right, on top, is the integral of the voltage divided by the sum of the inductance of the feed and load. Since the voltage divides inductively, we can calculate, from our knowledge of the inductance as a function of position, the voltage across the feed at any radial location. We can then plot the current as a function of voltage (characteristic plot) at any position along the feed. We show a characteristic at the bottom of the figure. This characteristic is typical of inductors driven by voltage pulses of the form $V = 0$, $t = 0$; $V > 0$, $0 < t < t_p$.

We then choose a criterion for trapping which could be $I > I_c$, I_{min} or I_p. We then multiply one of the characteristics of Fig. 4 (I_c, I_{min}, or I_p) by the local geometrical factor which we determine from the geometry. We then superimpose this characteristic on the characteristic for the inductor. Whether the feed will or will not be magnetically insulated will depend on whether the inductor characteristic falls above or below the characteristic we chose (I_c, I_{min}, or I_p).

The cross-hatched area of the figure shows where the inductor characteristic falls below the trapping criterion. In this region of the I-V plane, which maps onto a $r < t$ region of the feed, electrons will be lost to the anode.

As in the case of circuit analysis calculations, the criterion for magnetic insulation is somewhat arbitrary ranging between the most stringent $I \geq I_p$ for voltages below 1 MV and the less stringent $I \geq I_c$ for voltages above 1 MV. Local measurements of voltage and current losses are useful to establish what the trapping criterion ought to be.

5.1.2. Equivalent Circuit Formulation

Equivalent circuit formulations which model the feed as a transmission line with a voltage and current controlled shunt conductance are useful to establish when cutoff takes place in the feed. Creedon [25] has developed a differential formulation which can easily incorporate the equations which describe the time evolution of the inductance of an imploding plasma load. The advantage of this approach is that the calculations can be normalized against experiments with actual loads. The disadvantage is, of course, that there is no mechanism in the calculation to establish what the cathode current is (or conversely, what fraction of the current is carried in the space charge) and the choice of cutoff criterion is somewhat arbitrary.

Waisman [26] has generalized Bergeron's [27] equivalent circuit approach with a differential formulation of the circuit equations and allowing currents to divide between the metal conductor of the MITL and plasma formed on the cathode of the MITL. He incorporated the 1-D MHD equations of motion for this plasma to establish bounds on its velocity and to determine whether the magnetic pressure in the feed could stop the plasma. He compared results from his calculations with experimental measurements by Di Capua in 1 and 2 m MITLs [28, 29]. The average plasma velocities of 2.4×10^6 cm s^{-1}, which he obtained for aluminum plasmas were not sufficient to close the gap as it was observed in one experiment [30]. Moreover, at the time of peak current (130 ns into the pulse), the magnetic field in the gap was large enough to stop the highly conductive cathode plasma. He conjectured, however, that hydrogen plasmas could acquire higher velocities and close the gap in the shorter intervals observed in the experiment.

5.1.3. Particle Orbit Calculations and Drift Theory

To calculate electron trajectories in magnetically insulated feeds, we require an exact knowledge of the electric and magnetic fields in the feed. The presence of space charge in the feed alters the fields from their vacuum value. Near the cathode, space charge has a major role and the orbits in this region depend on the details of how the electric field, in the case of space charge limited flow, approaches zero. The electron current in the sheath also changes the profile of magnetic field across the gap from its vacuum configuration. Hence, particle orbit calculations and drift theory apply away from the cathode and the sheath, where space charge is not present.

When $c|\vec{B}| > |\vec{E}|$, the electrons execute Larmor orbits in the gap and drift towards the centerline. At the same time, when a ∇B is present, they drift towards the anode surface. It then becomes necessary to establish under what conditions electron trajectories intersect the anode. Drift calculations are useful for this purpose.

There are several approaches to obtain insight on the nature of particle trajectories in feeds which drive inductive loads. One approach is orbit calculations like the ones of Poukey [31] and Clauser [10] in time invariant fields where a ∇B is present. Another by Poukey [32] consists of orbit calculations in time varying magnetic fields where no ∇B is present. The last one by Shannon [33] consists of drift calculations in the presence of ∇B and time varying fields for three widely used feed geometries: parallel disks, bicones, and tangent spheres.

The electron orbits in the time invariant fields [10] intersect the anode at a radius which is proportional to the initial radius, the anode voltage and the square of the ratio of the vacuum impedance to the geometric impedance at the location where the electron is born. This simple result applies to parallel disk as well as bicone feeds.

A relativistic invariant of the motion of an electron is:

$$\mu' = \frac{\vec{P}' \cdot \vec{P}'}{2\, m_o |\vec{B}'|}$$

where the primed values correspond to quantities in a frame moving with a velocity $u_{eb} = \vec{E} \times \vec{B}/(\vec{B} \cdot \vec{B})$ with respect to the laboratory system such that

$$\gamma_{eb} = (1 - u^2_{eb}/c^2)^{-1/2} \quad , \quad \gamma' = (1 - v'^2/c^2)^{-1/2} \quad ,$$

$$\gamma = \gamma_{eb}\, \gamma' \text{ and } \vec{\beta} = \gamma_{eb} \vec{\beta}' \quad .$$

$\vec{P}'$ and $\vec{B}'$ are the kinematic momentum and magnetic field at the location where the electron is born. This invariant applies when changes in the field take place over times and distances which are large compared to the Larmor period and radius, respectively. Consequently, the drift velocity u_d arising from ∇B becomes:

$$u_d = \frac{\mu'}{q\gamma} (\vec{B}' \times \nabla |B'|)/(\vec{B}' \cdot \vec{B}') \quad .$$

Shannon [33] shows that in biconic and bispherical feeds driving inductive loads the radial velocity u_{eb} is a simple function of r and t, and is constant over the width of the gap at any given radial position. Consequently, the radial (or θ position) may be obtained from a straightforward integration of the velocity u_{eb}. The motion across the gap may then be obtained from integration of the equation for the drift velocity u_d where μ' is evaluated at the time and position of departure of the electron from the cathode. The result of the calculation is that electrons emitted early in the pulse at large radii will drift and reach the anode at small radii. McDaniel [10] has experimentally observed electrons striking the anode at small radii in PROTO II. He attributed this loss to ∇B drifts and reduced it by reintersecting the electron flow with a tapered cathode [34].

5.1.4. Particle-in-Cell Simulations

Particle-in-cell (PIC) simulations are considerably more difficult. The simplifications afforded by constant impedance geometries are no longer possible. The condition $\tau c/\ell > 1$ requires a reflection boundary condition at both ends of the feed, which is difficult to apply. Multiple reflections, which are unavoidable, also promote the growth of spurious waves and particle noise. Some results of early calculations [31] showed that at early times the electrons are not trapped, in agreement with predictions from the single particle orbit analysis. At late times, however, the single particle analysis and experimental results show that the electron flow in the feed is well trapped, while losses in the PIC simulation are still high.

5.2. POWER FLOW IN THE VICINITY OF THE LOAD

Power flow in the vicinity of the load has challenged experimentalists for the past several years. Large power flows across small areas with small gaps, plasma motion, small vacuum conductances, radiation environments, precise measurements in MV cm^{-1} and kT fields are only a few of the problems. Very few experimental results appear in the literature. Gilman's [35] description of vacuum power flow experiments in the PI-DNA PITHON accelerator illustrate many of these challenges. He observed efficient transport of $\simeq$ 4 MA to a radius of 3 cm, a large voltage spike in the feed at the time the array implodes and only a small fraction of the current appears to flow in the space charge in the vicinity of the load.

The last result is encouraging because the $\vec{E} \times \vec{B}$ drift velocity ($\sim E/B$) in the vicinity of the load may become very small when one attempts to transfer the magnetic energy stored in the feed to the load at the time of peak current. Therefore, the space charge power flow may be lost to the cathode before it reaches the load, unless the cathode recaptures the space charge flow electrons. Recapture is a difficult feat in rapidly varying megagauss, MV cm^{-1} fields.

5.3. GAP CLOSURE IN VACUUM FEEDS

The bridging of the vacuum feed gap by motion of plasmas formed at the electrodes sets a lower limit to the anode-cathode distance of MITLs in the vicinity of a radiating load. These plasmas could be formed by explosive emission at the cathode, electron deposition at the anode or by desorption and ionization of contaminants on the two electrodes by vacuum UV and soft x-ray irradiation.

A question which has received considerable attention is the difference in behavior between inductive short circuit loads [11] and dynamic loads which undergo an implosion (where $\dot{L}$ is present). Even though both loads exhibit the same electrical behavior at early times, efficient current transport into dynamic loads is more difficult due to an observed tendency of the feed to short circuit in the vicinity of dynamic loads. It may be possible that the vacuum UV produced during the evaporation and ionization phase of the dynamic loads, during the prepulse of the accelerator, will desorb and ionize materials on electrode surfaces. This is the motivation for Sincerny's research discussed below.

Spectroscopic measurements of Hinshelwood [36] on a field emission diode at MIT determined that cathode plasmas consist of cathode materials as well as surface impurities with the total amount of plasma increasing with pulse length and current density. More recent observations [37] indicate: a) that all species (H, C, $A\ell$) expand into the gap at the same velocity ($\sim$ 2 cm μs^{-1}) that is consistent with 4 eV H+ ions (the mechanism that would produce 40 ev $A\ell$ ions or 20 eV C ions is not clear at this time); and b) that the total plasma inventory (electrons/cm^2) is proportional to the total charge (Cb/cm^2) transported in the gap.

Observations of plasmas in the gaps of MITLs by Stinnett at SNLA [38] indicate that cathode plasma with a density of 10^{15} to 10^{16} cm^{-3} and a temperature of a few eV expands into the gap at a velocity of 1-2 cm μs. These plasmas have been observed to be a source of negative loss which are then accelerated to the anode surface.

Sincerny has studied plasmas produced by vacuum UV irradiation. Experimental results [39] show plasma velocities of 1 cm μs per J/cm^2 of incident radiation. As in the case of other investigations, the plasma position is independent of the material of the surface leading to the conjecture that the likely plasma source is diffusion pump oil absorbed on the surface. Another set of experiments [40] with a more intense source of radiation shoved blowoff densities of 5×10^{18} cm^{-3} at velocities as high as 10 cm μs^{-1}. They could be accounted for by irradiation of the surface by a 5 eV vacuum UV source 2 cm away. These experiments also showed an expansion velocity independent of the substrate material.

The gap closure may be partly alleviated by increasing the gap in the vicinity of the load and shielding the feed from the radiation environment. Wilson [41] has suggested that radiation from the cathode plasma may be sufficient to create an anode plasma which then closes the gap.

Another current loss may be due to negative ions which cross the gap. These have been observed by VanDevender [42] in long MITLs. The current loss due to ions in vacuum feeds driving imploding plasma loads, however, is expected to be small [43] even though the ion current density appears to scale as the cube of the electron current density carried across the gap [38].

VanDevender [43] has elaborated on an electrostatic closure model in which the bulk plasma accelerates through a charge exchange collision process. For a constant anode voltage V_o, the closure time τ for a gap d is:

$$\tau = \left(\frac{2}{V_o}\right)^{1/2} \frac{d}{C} \quad .$$

He obtained the value of $C = 190 \pm 65\ V^{-1/2}\ m\ s^{-1}$ from several experiments which did not, however, include imploding plasma loads. Data from imploding plasma loads to corroborate the theory is not available yet.

5.4. APPROACHES TO REDUCE THE INDUCTANCE OF VACUUM FEEDS THAT DRIVE IMPLODING PLASMA LOADS

Up to now, our discussions point out that the feed geometry plays a very important role in the efficiency of current transport from the insulator to the load. We also pointed out that large gaps in the feeds greatly simplify the current transport task. Large gaps, however, heavily burden the accelerator designer. They are invariably associated with larger inductances that increase electrical stresses in the dielectric region of the accelerator. Dielectric breakdown also limits the amount of current per unit perimeter the accelerator can deliver. Breakdown limits in the vacuum interface impose a heavy inductance penalty as well.

The approaches to minimize the inductance penalty of the power feed in the vacuum between the insulator and the load include:

a) Getting the insulator closer to the load.

b) Reduce the gaps in the vacuum.

c) Drive a single insulator with multiple power feeds.

d) Allow an opening switch to build up the current in the vacuum feed, thereby lowering the electrical stresses in the feed.

e) Improve the vacuum and precondition the vacuum feed surfaces to inhibit plasma formation.

One approach that has been suggested to get the insulator closer to the load is to use magnetic inhibition of insulator flashover. The magnetic field

of the currents in the vacuum feed can, in principle $\vec{E} \times \vec{B}$, drift electrons away from the insulator surface, thereby inhibiting the formation of the avalanche which breaks down the insulator. This process has been investigated theoretically by McDaniel [44] and Bergeron [45]. Experimental data reported by Di Capua [46] and VanDevender [47] shows that breakdown fields which are two to five times the commonly accepted values for negative angled insulators may be achieved with this technique. This technique may be used to reduce the height of insulator stacks, alleviating the convergence required in Type I transitions. Moreover, the insulator can be brought closer to the load which lowers the inductance of the feed. Attempts to use this technique in large accelerators, however, have not been very successful.

On the light of the discussion on gap closure, reduction of the gaps in vacuum does not appear to be a very promising approach to reduce the inductance of the feed.

Coupling of two or more feeds in vacuum with a convolute [48] can add the current from several feeds in the vicinity of the load. This coupling achieves two purposes: it allows more efficient utilization of the solid angle available for power flow and it reduces, by parallel connection, the inductance which may be achieved with a minimum gap. McDaniel [34] recently tested such a convolute on PROTO II, Miller [49] has proposed a post-hole convolute for Blackjack-6 and a convolute couples the upper and lower vacuum feeds in the Double-EAGLE accelerator [50].

Plasma erosion opening switches (PEOS) may hold the key to successful operation of MITLs and diodes with very small gaps by relieving the field stresses as the current builds up in the feed. Successful operation of these

switches has been reported by Stringfield [51], Sincerny [52], and Meeger [53]. Modeling of these switches [53, 54] suggests that magnetic cutoff of the electron flow plays a very important role in the opening of the switch.

6. CONCLUSIONS

While magnetic insulation is well on its way to fulfilling the promise of delivering multiterawatt/cm^2 power densities in particle beam and high energy density plasma drivers, some fundamental questions still remain:

a) Is the electron flow in the gap laminar, quasi-laminar or fully turbulent and the transitions between these flows?

b) Are lossless transitions possible on theoretical grounds and how can such transitions be practically implemented?

c) What are the mechanisms for gap closure?

d) How do surface conditions affect the behavior of an MITL?

e) Is there a fundamental limit to the power density that magnetic insulation can support?

The answers to these and other questions will be provided by the healthy combination of basic research, modeling, and empirical development that has advanced the field in the past.

REFERENCES

1. "Magnetic Insulation," IEEE Transactions on Plasma Science, PS-11, pp. 205-215, (1983). The second line in the fourth paragraph of this paper is a computer generated typesetting error that arose after the galleys were proofed. This line should be deleted.

2. C. W. Mendel, et al., "A Simple Theory of Magnetic Insulation from Basic Physical Considerations," Lasers and Particle Beams, 1, pp. 311-320 (1983).

3. C. W. Mendel, J. P. VanDevender, and G. W. Kuswa, "Determination of Line Voltage in Self-Magnetically Insulated Flows," in Proceedings 2nd IEEE International Pulsed Power Conference, Lubbock, TX, pp. 153-156; IEEE 79CH 1505-7 (1979).

4. M. S. Di Capua and D. G. Pellinen, "Magnetic Insulation in Triplate and Coaxial Vacuum Transmission Lines," PIFR-1009, Physics International Company, October 1978. Also issued as Sandia National Laboratories, Albuquerque (SNLA) as SAND80-7029 (1980).

5. J. P. VanDevender, "Long Self-Magnetically Insulated Power Transport Experiments," J. Appl. Phys. 50 (6), pp. 3928-3934 (1979).

6. "Particle Beam Fusion Progress Report, January through June 1981," SNLA, SAND81-1459 (1982).

7. J. M. Creedon, "Relativistic Brillouin Flow in the High ν/γ Diode," Journal of Applied Physics, 46 (7), pp. 2946-2955 (1975).

8. M. Y. Wang and M. S. Di Capua, "Operating Point of Long Magnetically Insulated Vacuum Transmission Lines," J. Appl. Phys. 51 (11), pp. 5610-5619 (1980).

9. G. Yonas, J. W. Poukey, K. R. Prestwitch, J. R. Freemen, A. J. Toepfer, and M. J. Clauser, "Electron Beam Focusing and Application to Pulsed Fusion," Nuclear Fusion, 14, pp. 731-740 (1974).

10. M. J. Clauser, B. G. Epstein, D. H. McDaniel, and J. W. Poukey, "Limits on Power Intensification in Magnetically Insulated Vacuum Transmission Lines," Paper 3R11, Annual Meeting of the Division of Plasma Physics of the American Physical Society, Bull. Am. Phys. Soc. 24, p. 978 (1979).

11. R. D. Genuario, M. Wang, T. S. Sullivan, and M. S. Di Capua, "Experimental and Computational Results for a Low Inductance Diode Assembly for Use on Imploding Plasma Experiments on the PITHON Accelerator," Bull. Am. Phys. Soc. 25 (8), p. 833 (1980).

12. J. M. Creedon, "Magnetic Cutoff in High-Current Diodes," Journal of Applied Physics, 48 (3), pp. 1070-1077 (1977).

13. C. W. Mendel, Jr., S. A. Slutz, and D. B. Seidel, "Analytic, Two-Dimensional, Time-Dependent Theory of Magnetically Insulated Electron Flow," SNLA, SAND82-1740 (1982); also: "A General Theory of Magnetically Insulated Flow," Phys. Fluids, 26, pp. 3628-3635 (1983).

14. E. L. Neau and J. P. VanDevender, "MITL--A 2-D Code to Investigate Electron Flow Through Nonuniform Field Region of Magnetically Insulated Transmission Lines," 2nd IEEE International Pulsed Power Conference, Lubbock, TX, pp. 479-482; IEEE 79CH 1505-7 (1979).

15. J. P. VanDevender, J. T. Crow, B. G. Epstein, D. H. McDaniel, C. W. Mendel, Jr., E. L. Neau, J. W. Poukey, J. P. Quintenz, D. B. Seidel, and R. W. Stinnett, "Self-Magnetically Insulated Electron Flow in Vacuum Transmission Lines," Physica, 104C (1981).

16. M. P. Desjarlais, et al., "Electron Dynamics in Magnetically Insulated Diodes," Proc. 5th International Conf. on High Power Particle Beams, pp. 190-193; UCRL-CONF830911 (1983).

17. A. Palevsky, "Generation of Intense Microwave Radiation by the Relativistic E-Beam Magnetron," (Experiment and Numerical Simulation), MIT Ph.D. Thesis, June 1980. C. L. Chang, et al., "Stability Theory of

Magnetically Insulated Electron Flow," Proc. 5th International Conf. on High Power Particle Beams, pp. 187-189; UCRL-CONF830911 (1983).

18. P. Champney, private communication (1976).

19. P. Spence, private communication (1977).

20. J. T. Crow and G. D. Peterson, "Terawatt Power Division and Combination Using Self-Magnetically Insulated Transmission Lines," IEEE 14th Pulsed Power Modulator Symposium, pp. 219-221, IEEE 80CH 1573-5 (1980).

21. J. T. Crow and G. D. Peterson, "Combination of PBFA-I Lines in a Disk Feed," Proceedings 3rd IEEE International Pulsed Power Conference, Albuquerque, NM, pp. 245-247, IEEE 81CH 1662-6 (1981).

22. D. B. Seidel, B. C. Goplen, and J. P. VanDevender, "Simulation of Power in Magnetically Insulated Convolutes for Pulsed Modular Accelerators," IEEE Power Modulator Symposium, pp. 222-226, IEEE 80CH 1573-5 (1980).

23. "Particle-Beam Fusion Progress Report, July 1980 through December 1980," SNLA, SAND81-0683 (1981); also, J. T. Crow and G. D. Peterson, "Recovery of Electron Sheath Current in Magnetically Self-Insulated Transmission Lines," IEEE Trans. on Plasma Science, PS-11, pp. 219-222 (1983).

24. C. Stallings, K. Nielsen, and R. Schneider, "Multiple-Wire Array Load for High-Power Pulsed Generators," Appl. Phys. Lett. 29 (7), pp. 404-406 (1976). Also, C. Stallings, K. Childers, I. Roth, and R. Schneider, "Imploding Argon Plasma Experiments," Appl. Phys. Lett. 35 (7), pp. 524-526 (1979).

25. V. L. Bailey, J. M. Creedon, B. M. Ecker, and H. I. Helava, "Intense Relativistic Electron Beam Injector System for Tokamak Current Drive," PITR-1382, USDOE DE-AM03-76SF00010/DE-AT03-76ET53019, (Interim Technical Report) (1981); also, J. Appl. Phys., 54, pp. 1657-65 (1983).

26. E. Waisman and M. Chapman, "Vacuum Transmission Lines in the Presence of a Resistive Cathode Plasma," J. Appl. Phys., 53 (1), pp. 724-730 (1982).

27. K. D. Bergeron, "Equivalent Circuit Approach to Long Magnetically Insulated Transmission Lines," J. Appl. Phys., 48 (7), pp. 3065-3069 (1977).

28. M. S. Di Capua, "Magnetic Insulation," PIIR-1-80, Physics International Company, San Leandro, CA (1980).

29. M. S. Di Capua, "Magnetic Insulation," PIIR-2-80, Physics International Company, San Leandro, CA (1980).

30. M. S. Di Capua and T. S. Sullivan, "Magnetic Insulation in Short Coaxial Vacuum Structures," Digest of Technical Papers, 2nd IEEE International Pulsed Power Conference, Lubbock, TX, pp. 483-86, IEEE 79CH 1505-7 (1979).

31. "Particle Beam Fusion Progress Report," SNLA, January 1979 through June 1979, SAND79-1944 (1980).

32. "Particle Beam Fusion Progress Report," SNLA, June 1979 through December 1979, SAND80-0974 (1981).

33. J. P. Shannon and F. S. Felber, "Implications of Electron Trajectories for Design of Magnetically Insulated Diodes," IEEE 14th Pulsed Power Modulator Symposium, Orlando, FL, IEEE 80CH 1573-5, pp. 214-218 (1980).

34. "Particle Beam Fusion Progress Report, January through June 1980," SNLA, SAND80-2500 (1981).

35. C. M. Gilman, G. H. Dahlbacka, R. Schneider, R. Stringfield, E. V. Buck, R. Dukart, P. Sincerny, and M. S. Di Capua, "Diagnostics Used on the PITHON Generator During Imploding Plasma Experiments," Proceedings 4th International Topical Conference on High Power Electron and Ion Beam Research and Technology, Palaiseau, France (1981).

36. D. Hinshelwood, "Cathode Plasma Formation in Pulsed High Current Vacuum Diodes," IEEE Trans. on Plasma Science, PS-11, pp. 188-196 (1983).

37. D. Hinshelwood, Ph.D. Dissertation, MIT (1984).

38. R. Stinnett, et al., "Small Gap Experiments in Magnetically Insulated Vacuum Transmission Lines," IEEE Trans. on Plasma Science, PS-11, pp. 216-219 (1983).

39. P. Sincerny, et al., "Plasma Blowoff from Electron Surfaces in the Presence of Vacuum Ultraviolet Radiation," IEEE Transactions on Plasma Science, PS-11, pp. 196-200 (1983).

40. P. Sincerny, et al., "Ablation of Electrode Surfaces in High Power Diodes," J. App. Phys., 54, pp. 7170-7175 (1983).

41. A. Wilson, E. Waisman, and M. Chapman, "Anode Heating by X-rays in High Power Diodes," Appl. Phys. Lett. 40 (11), pp. 949-950 (1982).

42. "Electron-Beam-Fusion Progress Report," SNLA, SAND76-0148 (1975).

43. J. P. VanDevender, "Power Flow for Vacuum Insulated Inductive Loads," Proceedings 3rd IEEE International Pulsed Power Conference, Albuquerque, NM, pp. 248-251; IEEE 81CH 1662-6 (1981).

44. K. D. Bergeron, "Theory of the Secondary Electron Avalanche at Electrically Stressed Insulator Vacuum Interfaces," J. Appl. Phys., 48, (7), pp. 3073-3080 (1977).

45. K. B. Bergeron and D. H. McDaniel, "Magnetic Inhibition in Vacuum," Appl. Phys. Let., 29 (9), pp. 534-536 (1976).

46. M. S. Di Capua, T. S. Sullivan, S. R. Ashby, and G. B. Frazier, "A Cast, Multistage, Diaphragm-Type, Hippodrome-Shaped, Magnetic-Flashover-Inhibited Insulator," Proceedings 4th International Topical Conference on High-Power Electron and Ion-Beam Research and Technology, Albuquerque, NM, pp. 252-55, IEEE 81CH 1662-6 (1981).

47. J. P. VanDevender, D. H. McDaniel, E. L. Neau, R. E. Mattis, and K. D. Bergeron, "Magnetic Inhibition of Insulator Flashover," J. Appl. Phys. 53 (6), pp. 4441-4447 (1982).

48. I. D. Smith, "Approaches to the Generation of Hundred Megampere Short Pulse Electron Beams," in Proceedings 1st International Conference on Electron and Ion Beam Research and Technology, Albuquerque, NM, pp. 472-489; SAND-76-5122, (1976).

49. A. R. Miller, "Sub Ohm Coaxial Pulse Generators, Blackjack 3, 4, and 5," Proceedings 3rd IEEE Pulsed Power Conference, Albuquerque, NM, IEEE 81CH pp. 1662-6 (1981).

50. G. B. Frazier, M. Di Capua, et al., "EAGLE and Double-EAGLE," Proceedings of the 4th IEEE Pulsed Power Conference, pp. 583-589; IEEE-83CH1908-3 (1983).

51. R. Stringfield, et al., "Experimental Investigations of Plasma Erosion Switches on the PITHON Generator," Proc. 5th International Conf. on High Power Particle Beams, pp. 277-281; UCRL-CONF-83-0911 (1983).

52. P. Sincerny, et al., "Operating Specifications for a Rod Anode, Low Inductance, High Power MITL," Proceedings of the 4th IEEE Pulsed Power Conference, pp. 478-481; IEEE-83CH1908-3 (1983).

53. R. A. Meeger, et al., "Vacuum Inductive Store/Pulse Compression Experiments on a High Power Accelerator Using Plasma Opening Switches," Appl. Phys. Lett., 42, pp. 943-948 (1983); also, "Application of Plasma Erosion Opening Switches to High Power Accelerators for Pulse Compression and Power Multiplication," Proc. 5th International Conf. on High Power Particle Beams, pp. 335-341; UCRL-CONF830911 (1983).

54. R. J. Kares, "Numerical Simulation of Erosion Switch Performance on the PITHON Generator," Proc. 5th International Conf. on High Power Particle Beams, pp. 272-276; UCRL-CONF830911 (1983).

FIGURE CAPTIONS

Figure 1. Curves relating the anode current, cathode current, and anode potential for an MITL [2]. F = G = 1. For example, for a 42 Ω coax operating at 1.75 MV, I_c = 0.8 MV/42 Ω = 19 kA and I_a = 2.8 MV/42 Ω = 67 kA. Currents agree with experimental data displayed in Fig. 7 of Ref. [1].

Figure 2. Electron orbits in a Type I transition. A $\partial\phi/\partial z > 0$ in the transition (a) increases the canonical momentum of the electrons so that orbits which were common cycloids before the transition (zero canonical momentum) become curtate cycloids (b). By energy conservation, the lower turning point of the orbit can at most reach the cathode. A small amount of v_z makes a large difference in the orbits. The anode potential V_0 = 1 MV anode current I = 54.3 kA are the same as in Fig. 1(d). We chose the geometrical factor at the exit of the transition to make the orbits of electrons born after the transition tangent at the anode (c).

Figure 3. Electron orbits in a Type II transition. A $\partial\phi/\partial z < 0$ in the transition (a) reduces the canonical momentum of the electrons so that orbits which were common cycloids before the transition become prolate cycloids (b). The flow separates from the cathode and reaches a larger radius into the feed, then electron flow launched after the transition (c). The anode potential V_0 = 0.25 MV and anode current I = 54.3 kA are the same as in Fig. 2(d) of Ref. [1], so orbits at the entrance of the transition just touch the anode (V_0 = 0.25 MV).

Figure 4. A 180° model of a post-hole convolute which parallel connects a tridisk feed into a bidisk feed. (a) The posts merge the current from the top anode, through holes in the cathode, with the current in the bottom anode. The cathode current in the upper surface of the cathode merges with the current in the bottom surface by flowing through the edges of the holes. Magnetic insulation must be maintained in this complicated structure. (b) Shows schematically the magnetic field configuration in the convolute.

Figure 5. Magnetic insulation and imploding plasma loads. (a) shows the voltage applied to the vacuum feed. (b) shows the current which is the integral of the voltage. (c) shows the characteristic obtained by plotting the current as function of voltage. In the beginning of the pulse, the current is below that required for trapping. Electrons are lost to the anode in the shaded portion of the pulse.

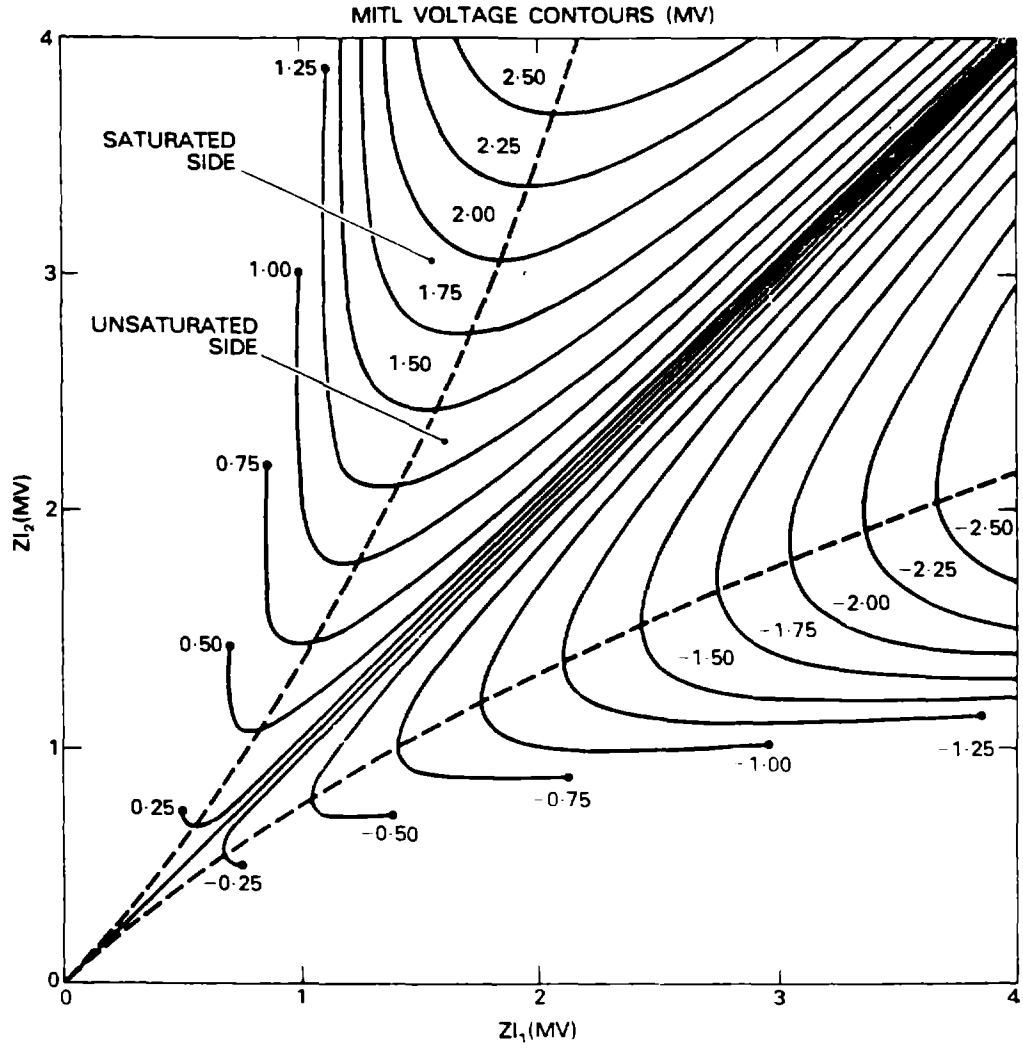

Figure 1. Curves relating the anode current, cathode current, and anode potential for an MITL [2]. F = G = 1. For example, for a 42 Ω coax operating at 1.75 MV, I_c = 0.8 MV/42 Ω = 19 kA and I_a = 2.8 MV/42 Ω = 67 kA. Currents agree with experimental data displayed in Fig. 7 of Ref. [1].

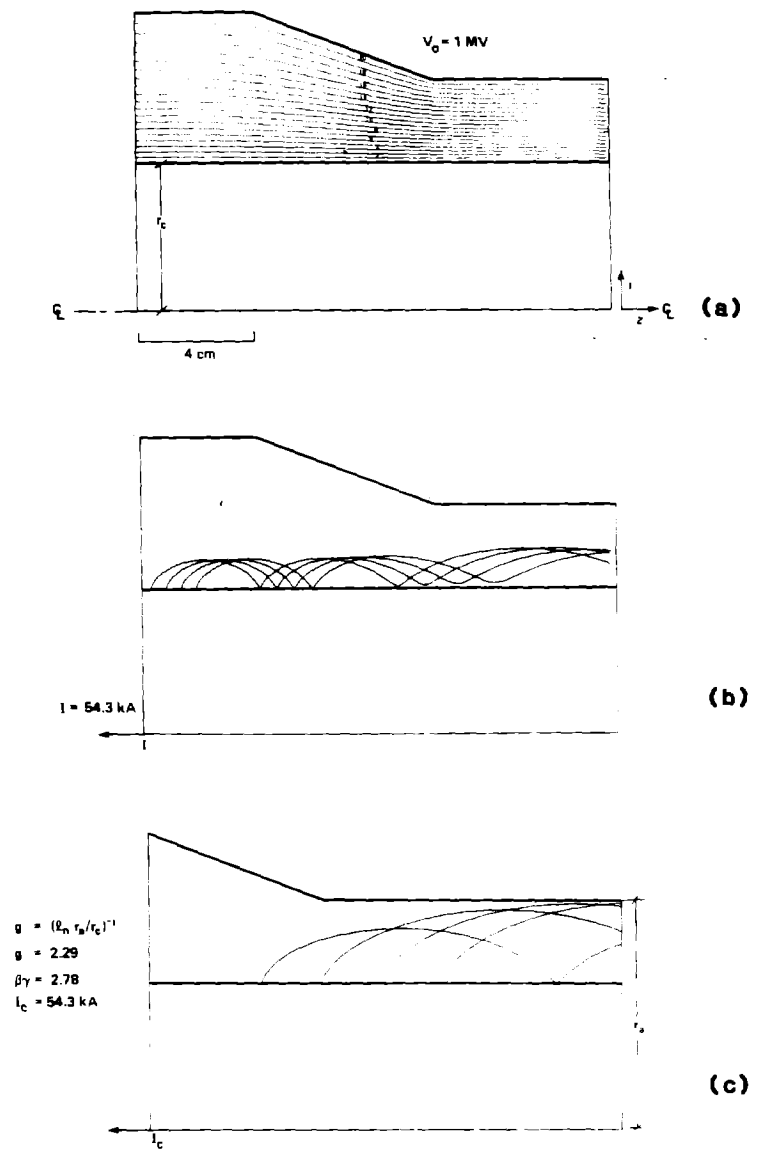

Figure 2. Electron orbits in a Type I transition. A $\partial\phi/\partial z > 0$ in the transition (a) increases the canonical momentum of the electrons so that orbits which were common cycloids before the transition (zero canonical momentum) become curtate cycloids (b). By energy conservation, the lower turning point of the orbit can at most reach the cathode. A small amount of v_z makes a large difference in the orbits. The anode potential V_0 = 1 MV anode current I = 54.3 kA are the same as in Fig. 1(d). We chose the geometrical factor at the exit of the transition to make the orbits of electrons born after the transition tangent at the anode (c).

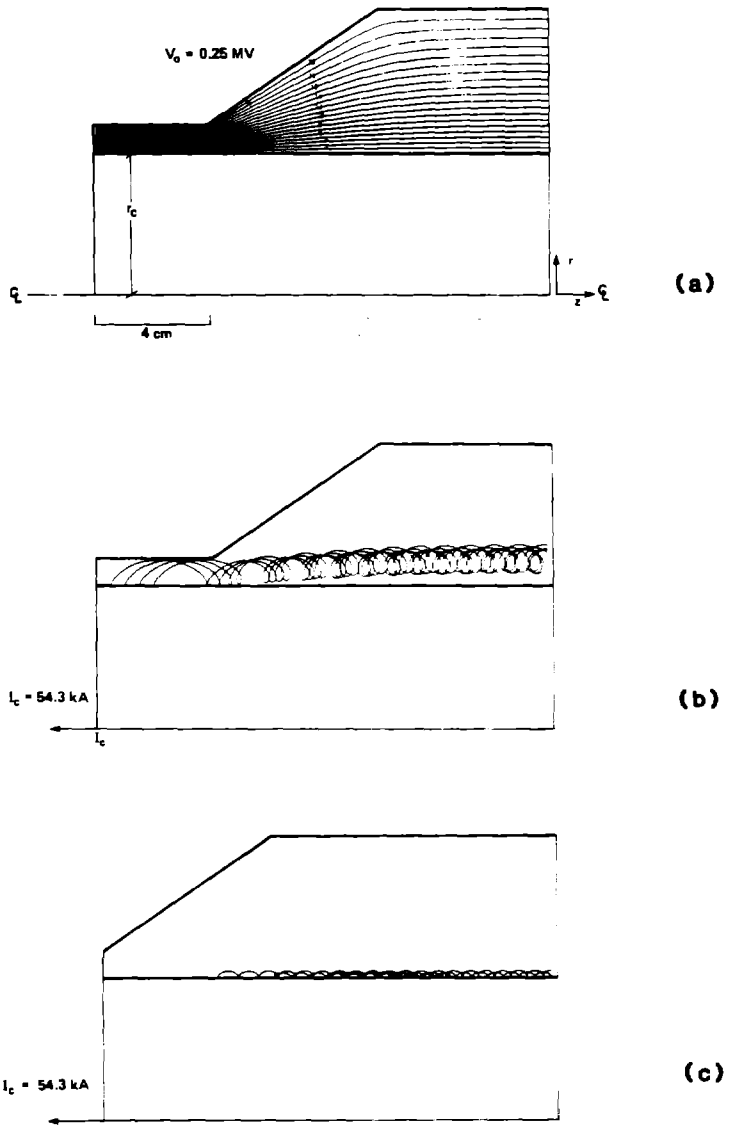

Figure 3. Electron orbits in a Type II transition. A $\partial\phi/\partial z < 0$ in the transition (a) reduces the canonical momentum of the electrons so that orbits which were common cycloids before the transition become prolate cycloids (b). The flow separates from the cathode and reaches a larger radius into the feed, then electron flow launched after the transition (c). The anode potential V_o = 0.25 MV and anode current I = 54.3 kA are the same as in Fig. 2(d) of Ref. [1], so orbits at the entrance of the transition just touch the anode (V_o = 0.25 MV).

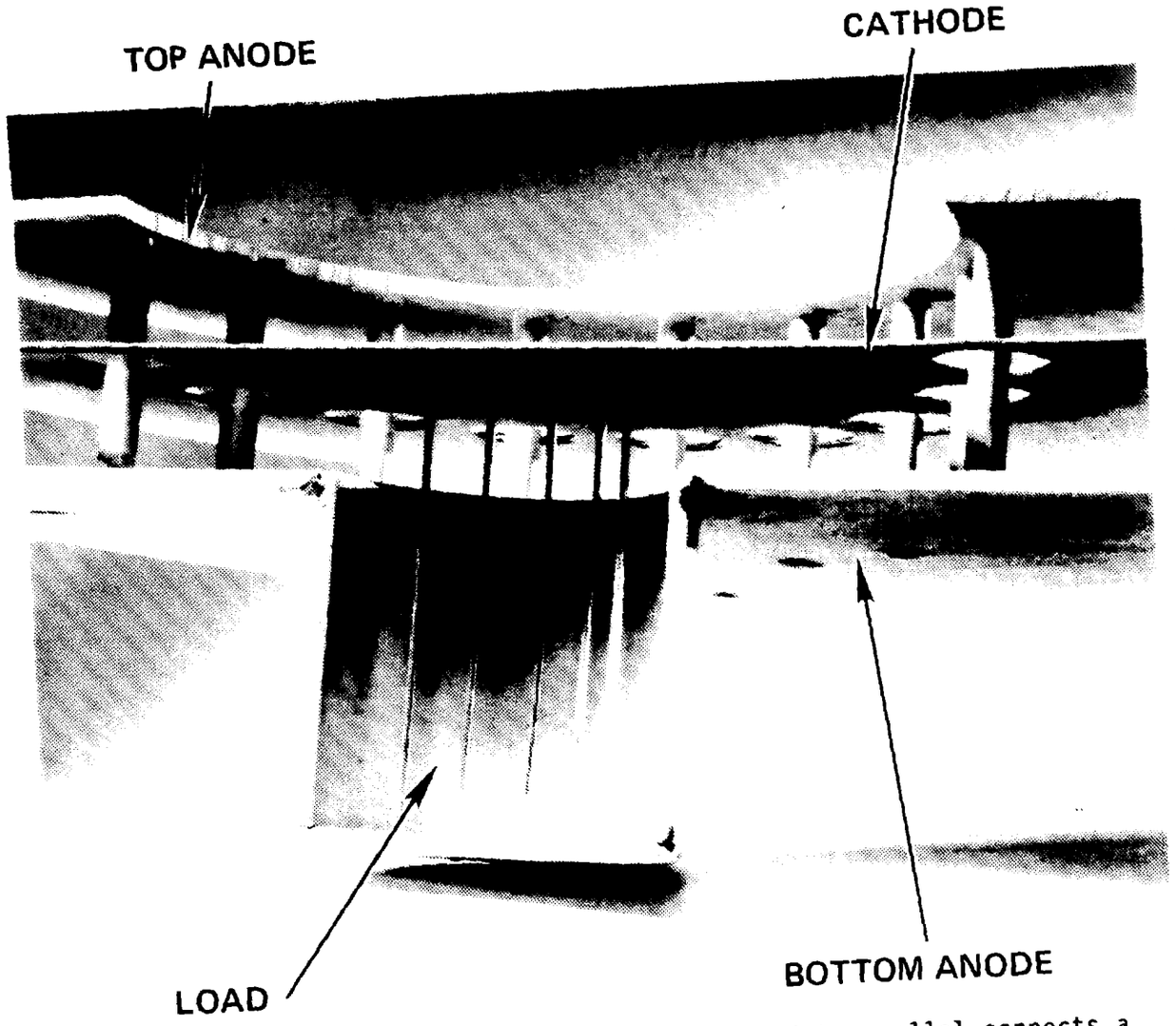

Figure 4a. A 180° model of a post-hole convolute which parallel connects a tridisk feed into a bidisk feed. (a) The posts merge the current from the top anode, through holes in the cathode, with the current in the bottom anode. The cathode current in the upper surface of the cathode merges with the current in the bottom surface by flowing through the edges of the holes. Magnetic insulation must be maintained in this complicated structure. (b) Shows schematically the magnetic field configuration in the convolute.

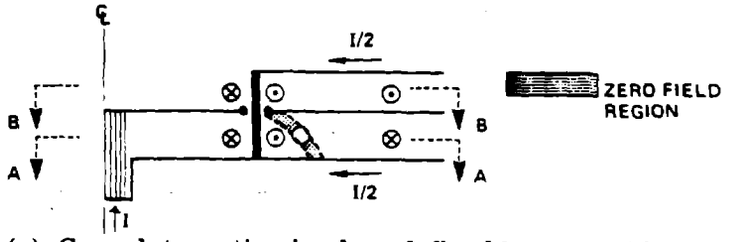

(a) Convolute section in plane defined by post midplane, which includes centerline.

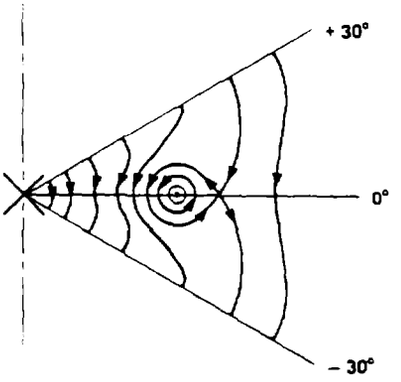

(b) Fields in A-A plane parallel to anode/cathode surfaces (six-fold symmetry).

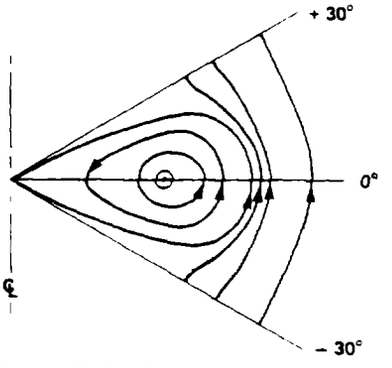

(c) Fields in B-B plane parallel to anode/cathode surfaces (six-fold symmetry)

Figure 4b.

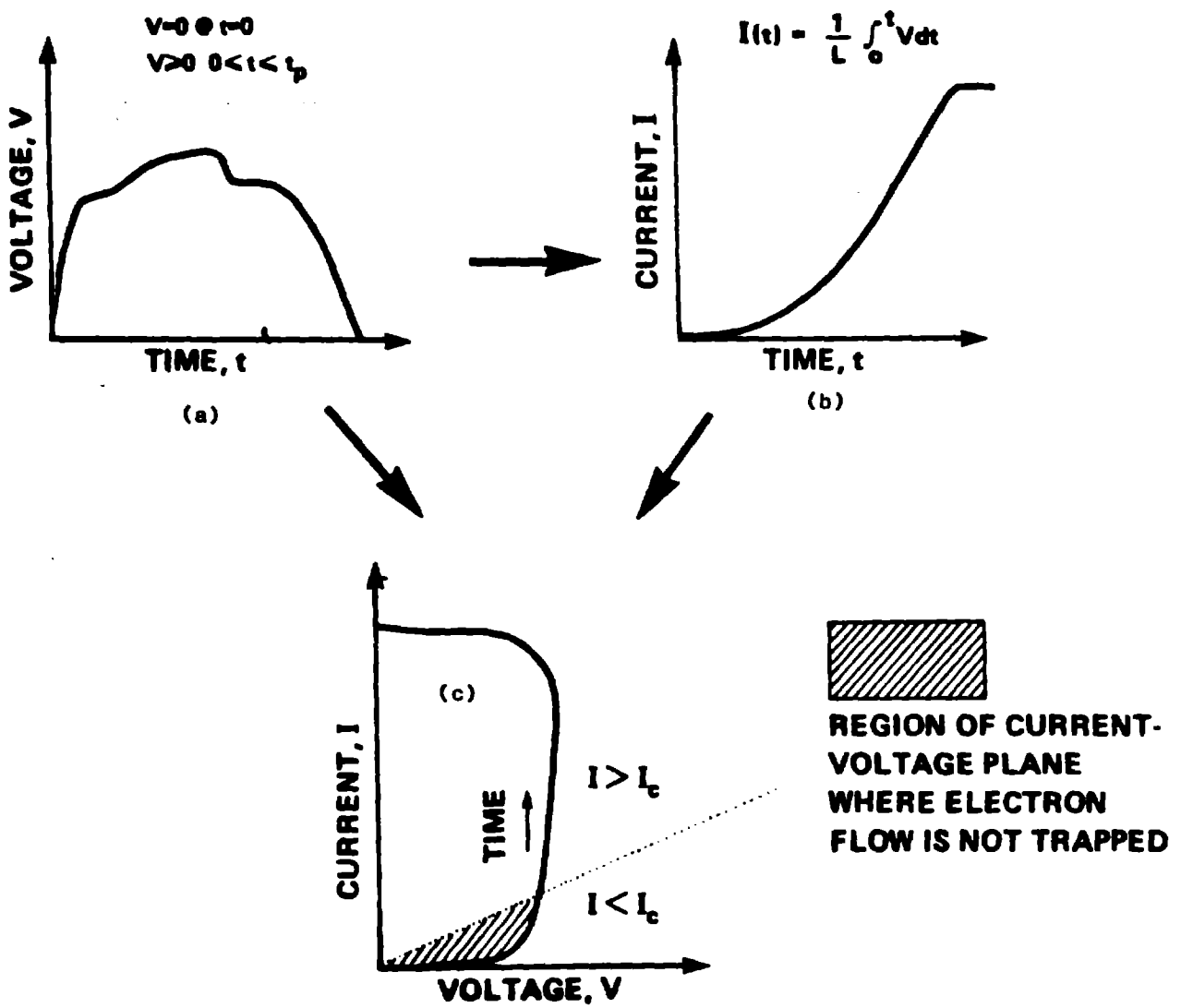

Figure 5. Magnetic insulation and imploding plasma loads. (a) shows the voltage applied to the vacuum feed. (b) shows the current which is the integral of the voltage. (c) shows the characteristic obtained by plotting the current as function of voltage. In the beginning of the pulse, the current is below that required for trapping. Electrons are lost to the anode in the shaded portion of the pulse.